Fitting range data to primitives for rapid local 3D modeling using sparse range point clouds

Kwon, Soon-Wook; Bosche, Frederic Nicolas; Kim, Changwan; Haas, Carl; Liapi, Katherine

Published in:
Automation in Construction

DOI:
10.1016/j.autcon.2003.08.007

Publication date:
2004

Document Version
Peer reviewed version

Fitting Range Data to Primitives for Rapid Local 3D Modeling Using Sparse Range Point Clouds

Soon-Wook Kwon [a]*, Frederic Bosche [a], Changwan Kim [a],
Carl T. Haas [a], Katherine A. Liapi [a]

[a] Department of Civil Engineering, The University of Texas, Austin, TX 78712, USA

Abstract

Techniques to rapidly model local spaces, using 3D range data can enable implementation of: (1) real-time obstacle avoidance for improved safety, (2) advanced automated equipment control modes, and (3) as-built data acquisition for improved quantity tracking, engineering, and project control systems. The objective of the research reported here was to develop rapid local spatial modeling tools. Algorithms for fitting sparse range point clouds to geometric primitives such as spheres, cylinders, and cuboids have been developed as well as methods for merging primitives into assemblies. Results of experiments are presented and practical usage and limitations are discussed.

Keywords: Sparse range point clouds, 3D workspace modeling, Fitting and matching objects, Merging objects

Introduction

Graphical workspace modeling can bring about improvements in safety while at the same time lessening the need for skilled workers to operate heavy equipment under a wide range of working conditions. There are two general modes in which graphical workspace modeling can be applied for equipment operations: (1) as interactive visual feedback while a piece of heavy equipment is being operated, or (2) as a tool for 3D graphical simulation. In the latter case, application of such a modeling technique can ultimately contribute to an equipment operator's sense of whether—and how—he/she should move before actually proceeding to do so. Research indicates that several different classes of operations that are performed on construction sites, such as earth moving, heavy lifting, and material handling, can be performed more safely and effectively by using graphical models of both the equipment and the workspace [3, 4, 11, 12, 15, 17, 18, 24]. Such advantages are further leveraged when applied to remote operations such as excavation in cofferdams and work below ground.

Three-dimensional laser-scanning systems are becoming popular tools for generating 3D models of construction sites [3]. These large, expensive range scanners (typically costing $30k–$100k apiece) are placed at various positions around the scene so that dense range-point clouds can be obtained from each view. Then, the individual range-point clouds are merged into a single, registered, comprehensive point cloud. Heuristic methods are used to extract the geometric information: edges, surfaces, features, etc. [19]. This is a time-consuming operation, since the algorithms often fail to completely and accurately represent the entire point cloud. As a result, human intervention is needed to redirect the algorithm and manually finish the task where the algorithm left off [22]. While these methods can produce very detailed models of the scanned

scene, which are useful for obtaining as-built drawings of existing structures, the burdens that they impose in terms of computation and data-acquisition time generally preclude the use of these types of laser systems on-site for real-time decision-making. Modeling times for these laser range scanners can be on the order of hours or even days. In addition, it is virtually impossible to perform automated path planning based on their output because of the exorbitant computational cost of considering each point of a surface in the vicinity of the equipment being used for such a task [9].

The dynamic nature of the construction environment requires not only that a real-time local-area modeling system be fast but also that it be capable of dealing with uncertainty and adjusting to changes in the work environment. The ability to cope with uncertainty is very important and is being recognized as the next logical step in the robotics field as well [2]. The aim of the research reported is to contribute elements to a method of rapid 3D workspace modeling that achieves an acceptable balance between the degree of human judgment required for its use and the efficiency of acquisition of the range data. Such an approach is expected to bring about reductions in both computational costs and processing time, and lead to a cost-effective robust approach suitable for field deployment and eventual commercialization.

Rapid 3D Modeling on Construction Sites

Characteristics of Rapid 3D Modeling

For effective rapid 3D workspace modeling, three dominant issues need to be considered: (1) types of range point cloud data and their acquisition, (2) the role and application of human judgment, and (3) efficient workspace representations.

Types of Range Point Cloud Data and Their Acquisition

Most workspace modeling applications in the construction industry use dense point cloud data (Cyrax, NIST, and Carnegie Mellon University). An outstanding example is a laser scanning system of Cyra Corporation that extracts 3D data points of the work environment and involves a semi-manually assisted 3D model regeneration method using point clouds [5]. Cyrax combines a high resolution distance measurement sensor with software that creates 2D drawings and 3D models that are exportable for industry standard CAD and graphical modeling (IGES, AutoCAD, DXF, Microstation DGN, ASCII, BMP, and JPEG). Another prominent 3D laser-scanning system, LADAR (for Laser Distance and Ranging), is being developed by the National Institute of Standards and Technology (NIST) for use in applications such as automated determination of operations to be performed by earth-moving equipment, 3D as-built modeling of construction sites, and material tracking systems [3, 25, 26]. Finally, the Robotics Institute at Carnegie Mellon University developed an application for laser range scanners which is an autonomous loading system [24], which uses two scanning-laser rangefinders: one to recognize and localize the truck, and the other to measure the soil face.

Although these systems' scanning process provides more precise as-built 3D models relatively faster than other traditional manual measurement and design systems, they still require days or weeks for the modeling process due to their data densities [20]. Such computationally intensive processing approaches may render the dense point cloud approach prohibitive with respect to real-time applications in the construction industry. An alternative approach based on objective driven data acquisition would target individual objects and clusters of objects, and scan them with the minimum number of range points required in practice to model them accurately and efficiently. This approach is termed "sparse" range point clouds approach here and in [16, 19].

In contrast to full area, “dense”, range point scanning, the use of sparse clouds requires on the order of minutes for data acquisition and local area 3D modeling.

The Role and Application of Human Judgment

As opposed to fully autonomous systems [8, 13, 14], humans are adept at recognizing objects, especially in cluttered scenes such as construction sites [14]. By incorporating human perception into the overall modeling enterprise, an objective driven, sparse point clouds approach has the potential to reduce not only the data-acquisition time but also the need for processing that is computationally intensive and/or expensive [4, 19]. Therefore, integration of the decision-making ability of a human operator with the capability of a robot to carry out certain tasks semi-automatically may be more practical than use of full automation on construction sites [6]. Figure 1 shows comparison between the objective driven data acquisition approach of the research reported here and fully automated data acquisition that is more characteristic of existing approaches.

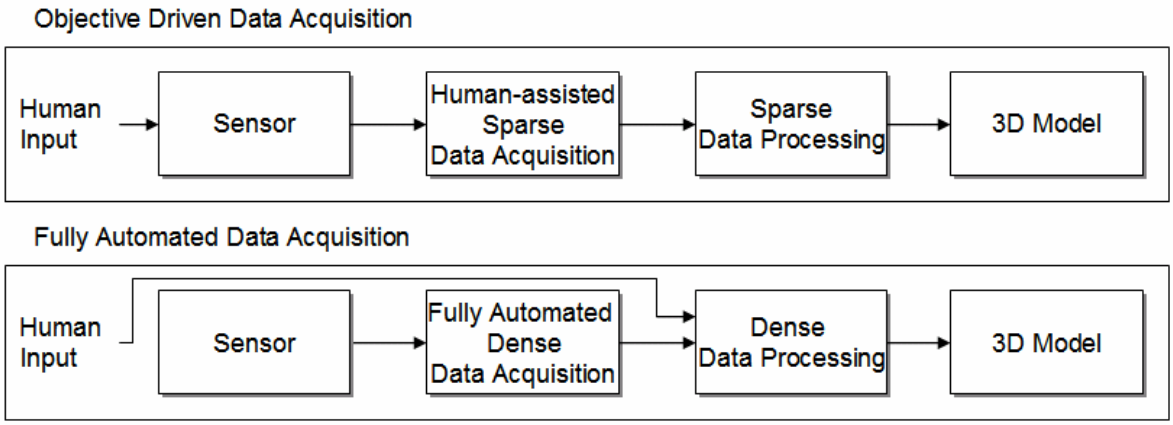

Figure 1: Comparison between objective driven data acquisition and fully automated data acquisition

Efficient Workspace Representation

In heavy-equipment operations, existence of a detailed local model is not critical. For example, in applications such as real-time obstacle avoidance, a set of simple polygons is most feasible. Neugebauer suggested that modeling of peripheral environments not directly related to a robot's task could be simplified by using a limited number of polygons, whereas workpieces actually handled by a robot should be modeled in more detail. The level of intricacy involved in operating the equipment should be considered in determining the level of detail needed for abstraction [21]. Thus, it is proposed that for objects that are not directly related to any equipment task, but still need to be modeled for purposes of obstacle avoidance or of heavy-equipment operation (*Peripheral Environment*), bounding algorithms can be employed to create models that completely encompass objects within the immediate environment without appreciable loss of workspace volume. For objects that are closely related to some task that is to be performed by the equipment (*Target Objects*), object fitting-matching-merging algorithms can be used to extract precise geometrical information from workplace scenes.

Comparison of Spatial Data Acquisition Techniques for World Space Modeling

The use of LADAR (Cyra and Carnegie Mellon University), FLASH LADAR (NIST), sparse point cloud and RFID systems lead to methods that achieve different results with different characteristics. It is useful to compare these methods using four main criteria related to the modeling potential of each:

- Precision and Accuracy: how well the model fits the original scene.
- Richness of the model derived with the approach: in terms of quantity and quality of information incorporated.
- Frequency of derived model updating

- Density of data used for modeling

Figure 2 roughly compares existing methods according to these criteria. While LADAR and RFID based systems are either very precise but slow, or fast but inaccurate, the sparse range point cloud method tends to achieve a compromise that is useful for some real-time field applications. It would probably be an order of magnitude less expensive than a LADAR or FLASH LADAR based approach.

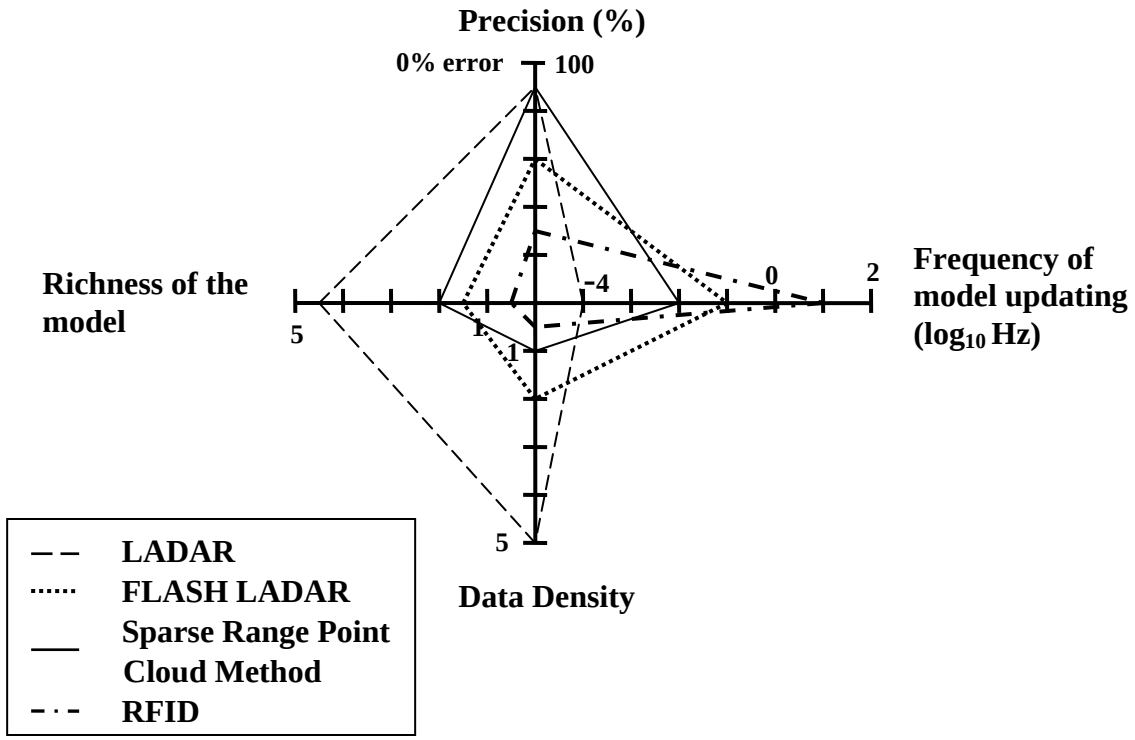

Figure 2: The Sparse Range Point Method in the world of Space Modeling

Process of Rapid 3D Modeling

For rapid local area 3D modeling using sparse range point clouds a process is followed as illustrated in Figure 3. This paper focuses on algorithms developed to execute the object modeling branch of the process flow chart (left hand column). The planar boundary and object

cluster modeling algorithms are described in McLaughlin, 2003 [19]. Combined, these processes lead to an efficient representation of the local work space. The range points are acquired using an inexpensive single axis laser range finder mounted on a pan & tilt unit.

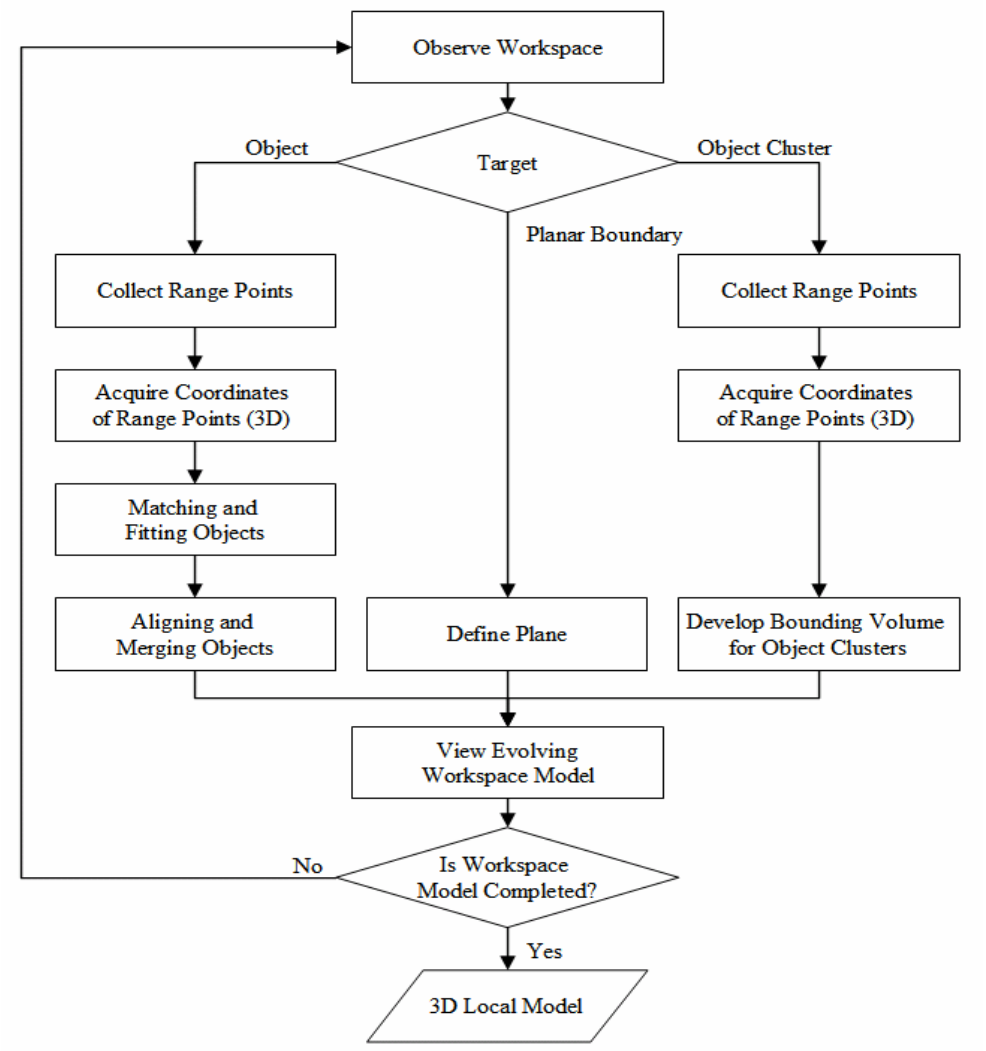

Figure 3: Process of Workspace Modeling

Target Objects & Human-Assisted Rapid 3D Workspace Modeling

With respect to the geometric primitives most frequently encountered in a construction site, a few types of objects can be used to model a wide range of construction scenes. Planar surfaces can be used for walls, ceilings, floors and other planar surfaced objects. Cuboids can be

used for fitting and matching structural objects such as columns, box-beams, and finishing objects. Cylinders can be used to fit and match chemical pipes, ventilation pipes, and concrete piles. Fitting and matching algorithms for cuboids and cylinders are presented and its experiments are discussed. Merging algorithms which is often required to represent target objects are also presented.

Primitives Fitting and Matching

Cuboids:

A bounded cuboid is described by a set of vertex points $vp = \{a, b, c, d, e, f, g, h\}$, and is composed of 6 surfaces. A bounded plane, one of the cuboid's six surfaces, is represented by a set of parameters $p = \{p_1, p_2, p_3, p_4\}$ that defines a plane, and a set of edge points, E, that lies in the plane and describes the vertices of the plane's boundary. The cuboid fitting method is used to find parameters for surfaces such as normals of all planes and vertex points. The cuboid method consists of four steps (Figure 6, 7, 8, 9, 10 and 11 show the results of the method step by step for a real object):

1) The *K*-nearest neighbors algorithm is used to segment points onto each surface of the cuboid. This algorithm finds the nearest two points in a 3D space by computing all distances from one scanned point to the other scanned points (see Figure 4, 5, and 7). After finding the two nearest neighbor points of each scanned point, the list of all three-point sets can be generated. Then the normal vector $(\vec{N}_x, \vec{N}_y, \vec{N}_z)$ for each set of three-point sets can be computed. Using these normals, the scanned points can be segmented by each cuboid surface (see Figure 8).

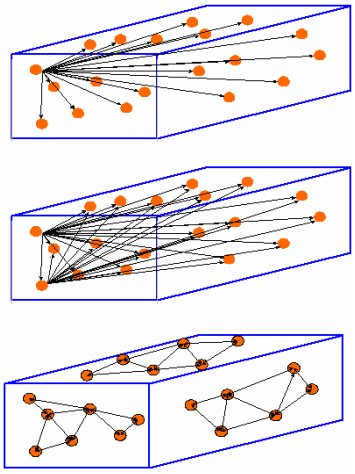

Figure 4: K-nearest Neighbors

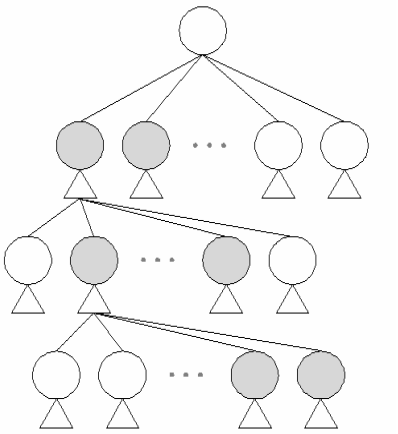

Figure 5: K-nearest Neighbors Tree

2) Plane optimization using the least squares method used to fit surfaces of the cuboid (see Figure 9). Using a linear equation, find the predicted *Z*, or $\hat{Z}_i = Ax_i + By_i + C$. The error term is defined as $\sum_{i=1}^{n}(Z_i - \hat{Z}_i)^2$. Given a set of data points *(x_i, y_i, z_i)*, determine the values of *A*, *B*, and *C* so that the predicted plane $\hat{Z}_i$ minimizes the sum of the squared residuals, $G = \sum_{i=1}^{n}(Z_i - \hat{Z}_i)^2$. This function is nonnegative and its graph is a hyperparaboloid whose vertex occurs when the gradient satisfies $\nabla G = (0, 0, 0)$. This leads to a system of three linear equations in which *A, B,* and *C* can be easily solved.

$$(0,0,0) = \nabla G = 2\sum_{i=1}^{m}[(Ax_i + By_i + C) - z_i](x_i, y_i, z_i) \tag{1}$$

$$Q = \begin{bmatrix} \sum_{i=1}^{m} x_i^2 & \sum_{i=1}^{m} x_i y_i & \sum_{i=1}^{m} x_i \\ \sum_{i=1}^{m} x_i y_i & \sum_{i=1}^{m} y_i^2 & \sum_{i=1}^{m} y_i \\ \sum_{i=1}^{m} x_i & \sum_{i=1}^{m} y_i & \sum_{i=1}^{m} m \end{bmatrix} \quad n = \begin{bmatrix} A \\ B \\ C \end{bmatrix} \quad d = \begin{bmatrix} \sum_{i=1}^{m} x_i z_i \\ \sum_{i=1}^{m} y_i z_i \\ \sum_{i=1}^{m} z_i \end{bmatrix} \tag{2}$$

$$n=Q^{-1}d \tag{3}$$

3) Intersecting edge line found between two surfaces and the vertices (see Figure 10 below). The line of intersection of two planes can be found by solving the two linear equations representing the planes. After applying these equations to three surfaces of the cuboid, we can find three intersection edges. Therefore, a vertex of a cuboid can be obtained from those three edges.

4) Point projections were used to compute parameters (see Figure 11). It is assumed that two points, (x_1, y_1, z_1), (x_2, y_2, z_2), are selected from the optimized plane. The size of the cuboid can be determined by computing the distance from each edge to the farthest point on a certain surface. The distance d from point K to a line defined by the end point P_1 and the direction V can be found by calculating the magnitude of the component of K-P_1 that is perpendicular to the line. The squared distance between the point K and the line can be found by subtracting the square of the projection of K-P_1 in the direction V from the square of K-P_1. This provides us below equations:

$$d^2 = (K-P_1)^2 - [proj_D(K-P_1)]^2 \tag{4}$$

$$= (K-P_1)^2 - [\frac{(K-P_1)\cdot V}{V^2}V]^2$$

$$= (K-P_1)^2 - \frac{[(K-P_1)\cdot V]^2}{V^2}$$

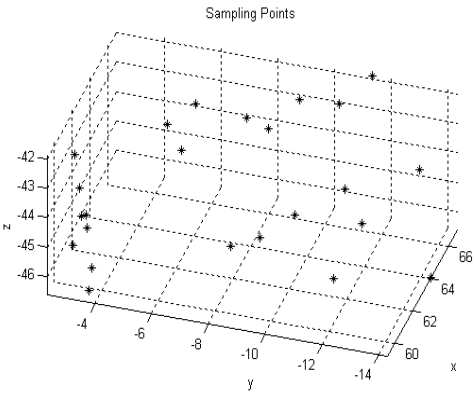

Figure 6:Scanned Points

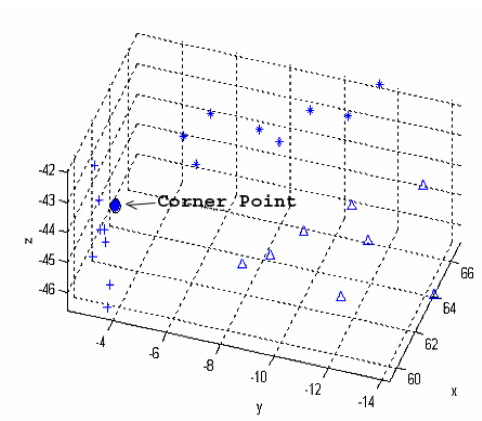

Figure 7: Points Projected on Optimized Surfaces

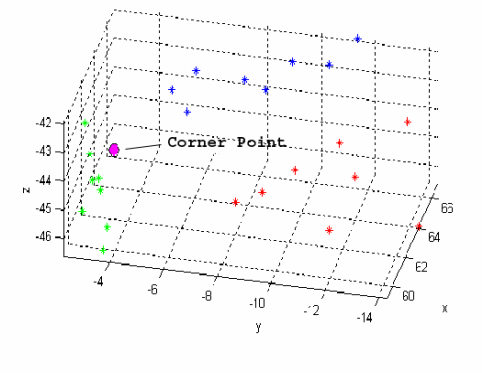

Figure 8: Segmented Points

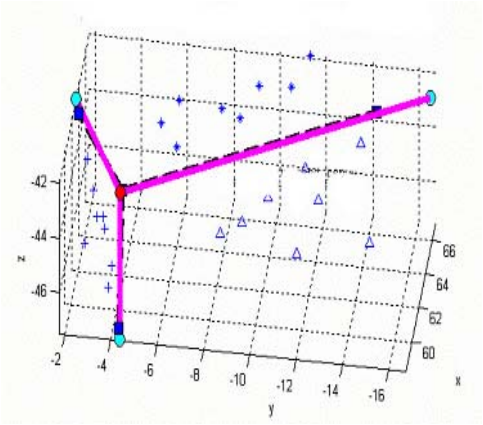

Figure 9: Computed Edges

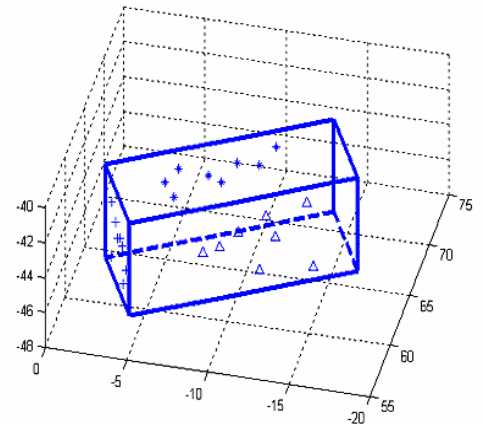

Figure 10: Fitted and Matched Cuboid

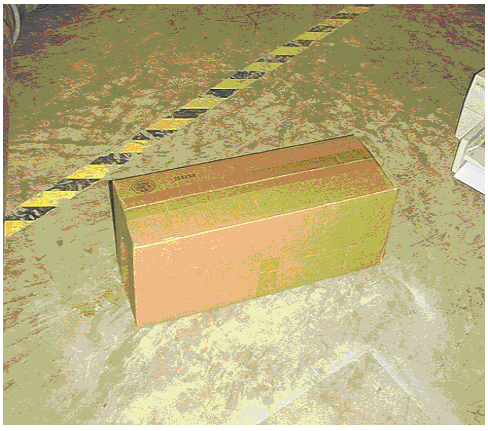

Figure 11: Actual Object

A second method is developed based on the previously explained cuboid fitting and matching method but applies when only two surfaces are visible. The process includes:

1. Data acquisition from the laser range finder
2. Segmentation of the scanned points into two surfaces of the cuboid using the k-nearest neighbors method
3. Edge detection
4. Point projection and computation of parameters of the cuboid

When only two surfaces are visible, the third surface must be automatically generated using the surface locations and axis normals of the two original ones. Figure 12, 13, 14, and 15 show the results of this method for an example.

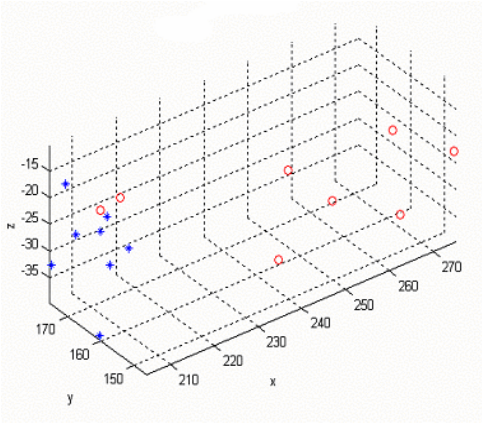

Figure 12: Result of Point Segmentation

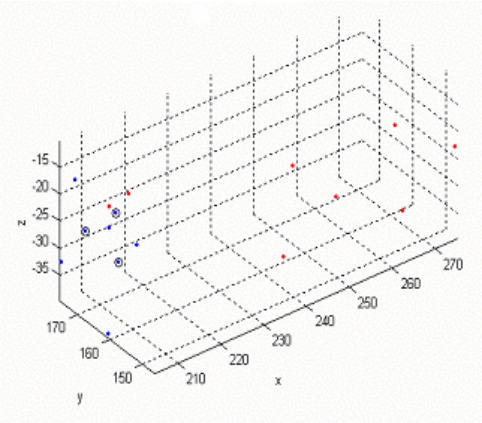

Figure 13: Representing Points of Two Surfaces

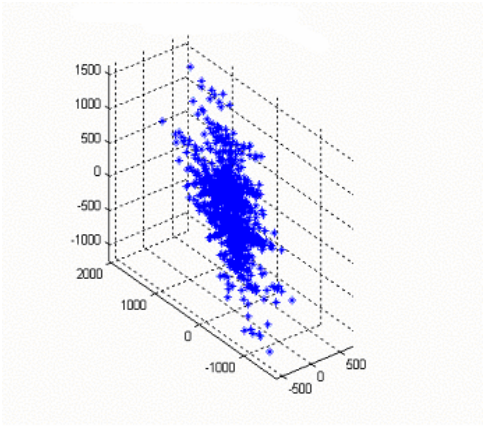

Figure 14: Clusters of Normals

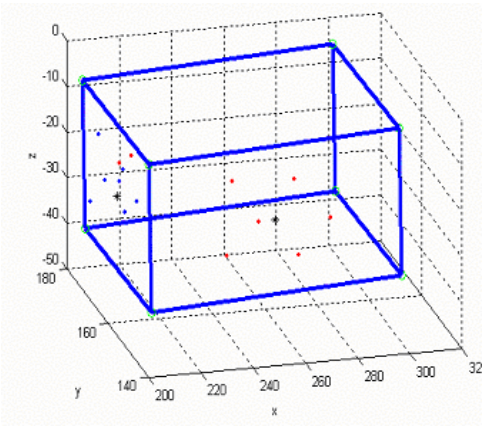

Figure 15: Fitted Model

Cylinders:

This section describes the fitting and matching method for cylinders. Four parameters define a bounded cylinder: an axis vector b; a center point $c_r = (X_c, Y_c, Z_c)$; a scalar radius r; and a length. These parameters must be calculated from a set of scanned points $d = \{(X_i, Y_i, Z_i)\}$ that define the boundary of the cylinder. The Figure 16 shows the process for fitting and matching cylinders that is presented more in details below.

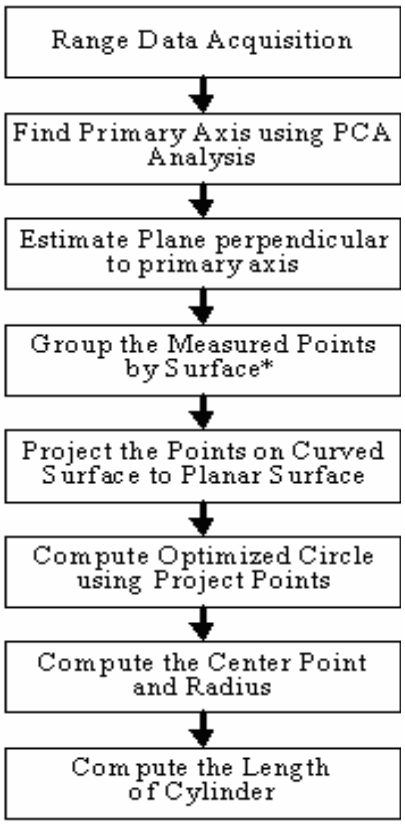

Figure 16: Process for Fitting and Matching Cylinders

Duda's Principal Components Analysis (PCA) was used to determine the primary axis of a cylinder [7]. PCA is a distribution-based ordination method in which the distances between sites in an ordination diagram are correlated with multi-dimensional distribution. PCA assumes that all vectors in a set of *n* dimensional samples $a_1 \ldots a_n$ can be explained by a single vector a_0. The vector a_0 is derived using the least squares method, in which the sum of the squared distances between a_0 and the various a_k are minimized. We define the square-error criterion function $F_0(a_0)$ by:

$$F_0(a_0) = \sum_{b=1}^{n} (a_0 - a_b)(a_0 - a_b)^t \tag{5}$$

$$p = \frac{1}{n} \sum_{b=1}^{n} a_b \tag{6}$$

$$F_0 = \sum_{b=1}^{n}((a_0 - p) - (a_b - p))((a_0 - p) - (a_b - p))^t \tag{7}$$

Projecting the sample data onto a line through the sample mean, one-dimensional representation can be computed. If we let e be a unit vector of the line direction, the line equation is

$$a = p + de \tag{8}$$

Scalar d is the distance between the sample data and the sample mean p. We can find the coefficients d_k by minimizing the squared criterion function.

$$F_0(d_1,...,d_n,e) = \sum_{b=1}^{n}(d_b e - (a_b - p))(d_b e - (a_b - p))^t \tag{9}$$

$$d_b = e^t(a_b - p) \tag{10}$$

The best direction e of the line can be found by solving scatter matrix U, which is defined by

$$U = \sum_{b=1}^{n}(a_b - p)(a_b - p)^t \tag{11}$$

$$F_1(e) = -e^t U e + \sum_{b=1}^{n}(a_b - p)(a_b - p)^t \tag{12}$$

LaGrange multipliers can be used to maximize the e^tUe, which is subject to the constraint $||e||=1$. Let φ be an undetermined multiplier. We can do the differentiation of v with regard to e, getting:

$$v = e^t U e - \phi(e^t e - 1) \tag{13}$$

$$\frac{\partial u}{\partial e} = 2Ue - 2\phi e \tag{14}$$

By setting the gradient vector equal to zero, we see that *e* should be an eigenvector of the scatter matrix (see Figure 17 for an application example). The eigenvector will be the primary axis of the hyper-ellipsoid that can be obtained by reducing the dimensionality of the feature space and by restricting attention to the directions along the scatter of the cloud [23, 27, 28].

$$Ue = \phi e \tag{15}$$

After finding the primary axis of a cylinder, estimated planar surfaces can be generated on the top and bottom of a cylinder. As can be seen in Figure 18 and Figure 19 for an example, by projecting the points of the curved surface onto the estimated planar surfaces, the radius and center point of the cylinder can be estimated. The process for computing optimized radius applies the curve fitting method to identify an optimized circle using measured points.

1. Move the axes to the intersection between the primary axis of the cylinder and planar surface of the cylinder using the transformation matrix.
2. Rotate the transformed axes to match with the primary the axis of the cylinder.
3. Project all the points on the curved surface into the planar surface.
4. Find the optimized center point of the cylinder to fit the cylinder

The Gander, Golub, and Steebel algorithm for computing optimized circle in three-dimensional space was used for this method as a fast method of circle fitting [10]. The center point and radius of a cylinder can be derived using the following formula

$$F(x) = kx^T x + l^T x + m = 0 \tag{16}$$

The coefficients *k, l,* and *m* are computed from a linear system of equations *Cv=0* for the coefficients v = $(k, l_1, l_2, m)^T$, such that

$$B = \begin{pmatrix} x_{11}^2 + x_{12}^2 & x_{11} & x_{12} & 1 \\ \vdots & \vdots & \vdots & \vdots \\ x_{n1}^2 + x_{n2}^2 & x_{n1} & x_{n2} & 1 \end{pmatrix} \tag{17}$$

In general, when the system of nonlinear equations is greater than 3, the solution to the system is over-determined. In order to solve the over-determined system, $Bv=0$ where v is chosen to minimize $\|r\|$.

$$\|Bv\| = \min \tag{18}$$

The center point and the radius are obtained $w=(w_1, w_2)$. This has the limitation of not providing the best fit in a geometric sense, but is a useful starting point for minimizing the geometric distance.In order to find the least squares solution for a nonlinear equation it is necessary to minimize the distance $d_1^2 = (\|w - x_i\| - r)^2$ so that:

$$\sum_{i=1}^{n1} d_i(v^2) = \min \tag{19}$$

$$I(v) = \begin{pmatrix} \frac{v_1 - x_{11}}{\sqrt{(v_1 - x_{11})^2 + (v_2 - x_{12})^2}} & \frac{v_2 - x_{12}}{\sqrt{(v_1 - x_{11})^2 + (v_2 - x_{12})^2}} & -1 \\ \vdots & \vdots & \vdots \\ \frac{v_1 - x_{n1}}{\sqrt{(v_1 - x_{n1})^2 + (v_2 - x_{n2})^2}} & \frac{v_1 - x_{n2}}{\sqrt{(v_1 - x_{n1})^2 + (v_2 - x_{n2})^2}} & -1 \end{pmatrix} \tag{20}$$

The set of points obtained while minimizing the algebraic distance can be iteratively substituted into $I(v)$. It obtains the best fit circle with center w and radius r (see Figure 20 for an application example).

Figure 17, 18, 19, 20, 21, and 22 display an example of cylinder fitting and matching.

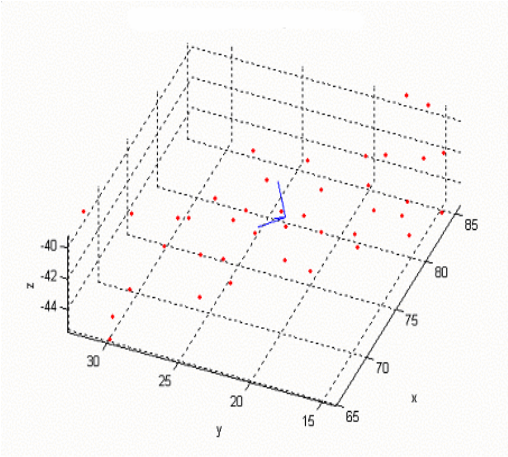

Figure 17: Scanned Points

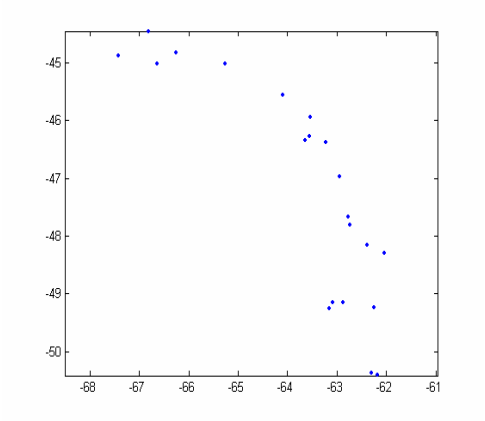

Figure 18: Circle Fitting Result

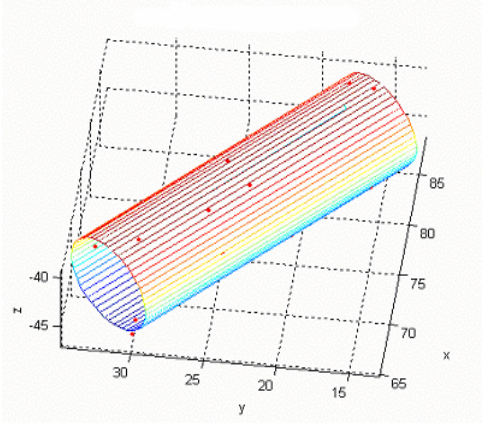

Figure 19: Fitted and Matched Model

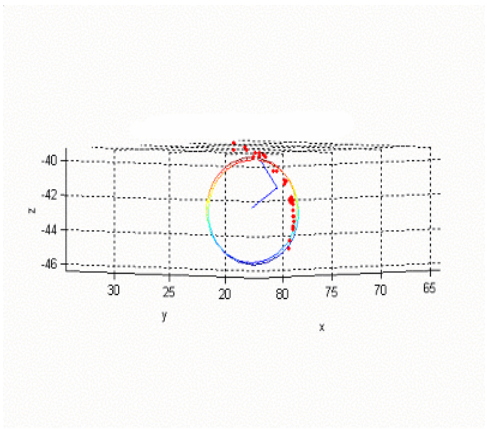

Figure 20: Projected Points before Circle Fit

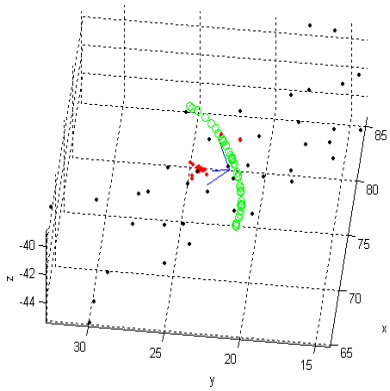

Figure 21: Result of Fitting and Matching

Figure 22: Pipe to be modeled

Experimental Results of Primitive Fitting and Matching

Experiments were performed to determine how accurately and rapidly the fitting and matching algorithms could build workspace models. An experimental test bed was set up of objects (cuboids and cylinders) with various dimensions. The number of points measured for each object was another parameter that has been varied during the experiments.

The key results are:

- For cylinders, the ratio $\frac{Length}{Diameter}$ strongly affects the accuracy of the modeling process: the higher, the more accurate.
- The bigger the cylinder, the more points are necessary to accurately model it (from 20 to 40 points).
- Cylinders can be modeled with a 1% to 5% precision error.
- A minimum of 30 points is needed to get accuracy of location, orientation, and sizes of cuboids.
- Cuboids can be modeled with a 1 to 2% precision error.
- Processing time is about a second, and data acquisition time depends on the ergonomics of the hardware.

Primitives Merging and Compliance Checking

Target objects often require not to be modeled with one but with many primitives. This is due to the fact that, by only modeling the primitives, they association is lost. Simple set membership for group transformations would be acceptable for many applications, however merging primitives can (1) improve visualization, (2) help reduce overall modeling errors, and (3) allow useful information to be associated with the primitives, or merged primitives. IN fact,

merging and compliance checking can be seen as graphic analogy to the spell check and grammar check functionalities in MS Word TM

For example, the dimensions of the primitives obtained with the previously described algorithms may be corrected by comparing contiguous elements of an object because they probably share some of these dimensions. For instance, the two diameters of scanned pipes known to be contiguous in a pipe spool can be equalized. The new value may be calculated as the closest standard value allowed for pipes. Not only the primitives' dimensions, but their orientation may be corrected using relationship information, in a form of compliance checking.

Merging may mean two things. First, merging may mean "grouping the primitives belonging to a same object". This can be very useful while considering the readability/clarity of screen-displayed modeled environment. Indeed, if it is known that the scanned primitives belong to two different objects, two different colors can be chosen to distinguish them. In the below, the comparison between the steps 1 and 2 shows how the relationship information can definitely help the user understanding a model, especially in the case of complex scenes.

Secondly, merging may mean "grouping and changing the primitives' dimensions ot other properties to better model an object". More interesting than choosing a color per object, it would be useful to connect the primitives graphically in order to obtain clearer and more accurate as-built models. Using merging process, step 3 in better illustrates that the scanned scene in step 2 is a structure, a pipe spool, a tank, and a chimney.

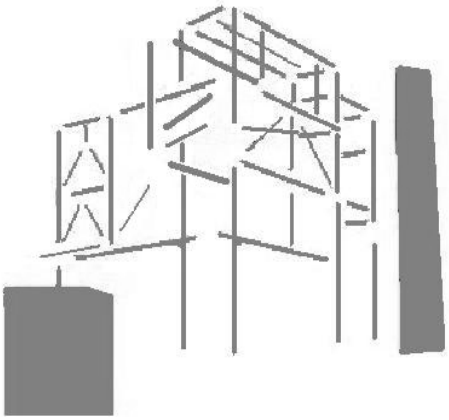

Step 1: No Object Recognition Process

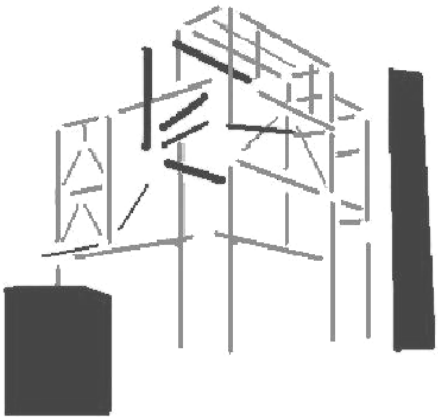

Step 2: Only Object Distinction Process

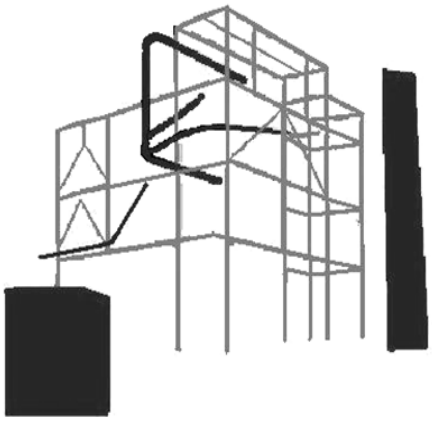

Step 3: Object Distinction and Object Reconstitution Processes

Picture of the Scanned Scene

Figure 23: How merging primitives can improve model display

Research is currently underway and algorithms have been or are still being developed for developing merging capabilities. These algorithms are reported in Bosche et al. [1].

Conclusions & Recommendations

A rapid 3D modeling approach that combines human recognition and a simple laser range finder has been developed. The short modeling times possible (minutes per scene) and the relatively small errors obtained in the modeling of primitives (usually no more than 5 percent for cylinders and cuboids) show that this method can be used to model construction-site objects at a

sufficiently rapid rate and with reasonable accuracy. This method is computationally efficient and suitable for use in applications such as safety enhancement in equipment control. It is also acceptable for generating construction as-builts.

This new approach to graphical workspace modeling is still in the outdoor testing stage. The merging algorithms and a graphical user interface are still being developed. Consequently, even if the principle of using "rapid 3D human-assisted modeling using sparse range points" is validated, further effort is needed to yield a product that could effectively be used on construction sites. Nonetheless, this method shows promise as a means of rendering accurate graphical models in short order.

Acknowledgements

This paper is based on the research funded by the National Science Foundation (Grant no. CMS-0000137) and National Institute of Standards and Technology (Grant no. NA1341-02-W-0742). The authors gratefully acknowledge their financial support and encouragement throughout this study.

References

[1] F. Bosche, C. Kim, S. Kwon, C. Haas, K. Liapi, "Primitives Merging for Rapid 3D Modeling", submitted to the *20th International Symposium on Automation and Robotics in Construction (ISARC)*

[2] M. Brady, Editorial Note, *International Journal of Robotics Research*, 18(11), 1999

[3] G. Cheok, W. Stone, "Non-intrusive Scanning Technology for Construction Assessment", *Proceedings of the 16th International Symposium on Automation and Robotics in Construction (ISARC)*, Madrid, Spain, Sep. 22–24 1999, pp. 645–650

[4] Y. Cho, C. Haas, K. Liapi, S.V. Sreenivasan, "A Framework for Rapid Local Area Modeling for Construction Automation", *Journal of Automation in Construction*, 11(6), pp 629-641, 2002

[5] Cyra Technologies, <http://www.cyra.com>, 2003

[6] P. Duda, D. Hart, D. Stork, "Pattern Classification," *Wiley-Interscience; 2nd edition*, October, 2000

[7] "Denver Gets Bag Handle", *Engineering New Records*, 233(7), 1993, p 10.

[8] Faugeras, M. Hebert, "The Representation, Recognition, and Locating of 3D Objects", *International Journal of Robotics Research*, 5(3), pp 13-51, 1986.

[9] T. Feddema, C. Little, "Rapid World Modeling: Fitting Range Data to Geometric Primitives", *Proceedings of the IEEE International Conference on Robotics and Automation*, vol. 4, pp. 2807–2812, 1997.

[10] Q. Gander, G.H. Golub, R. Strbel, "Fitting of Circles and Eclipse-Least Square Solution," Technical Report 217, Institute fur Wissenschaftliches Rechnen, ETH Zurich, June 1994

[11] C. Haas, M. Skibniewski,, E. Bundy, History of Robotics in Civil Engineering, Microcomputers in Civil Engineering, 10(5), pp 371-381, 1995.

[12] X. Huang, L. Bernold, "CAD Integrated Excavation and Pipe Laying", *Journal of Construction Engineering and Management*, 123(3), pp. 318-323, 1997

[13] D.P. Huttenlocher, S. Ullman, Recognizing Solid Objects by Alignment with an Image, *International Journal of Computer Vision*, 5(2), pp 195-212, 1990

[14] Johnson, O. Carmichael, D. Huber, M. Hebert, "Toward a General 3D Matching Engine: Multiple Models, Complex Scenes, and Efficient Data Filtering", *Proceeding of Image Understanding Workshop*, Monterey, pp 1097-1107, 1998

[15] Y.S. Kim, C. Haas, "A Model for Automation of Infrastructure Maintenance using Representational Forms", *Journal of Automation in Construction*, 10(1), pp 57-68, 2000

[16] S. Kwon, C. Haas, K. Liapi, S.V. Sreenivasan, "Human-assisted Object Fitting to Sparse Cloud Points for Rapid Workspace Modeling in Construction Automation", *Proceedings of the 19th International Symposium on Automation and Robotics in Construction (ISARC)*, Washington D.C., U.S.A., Sep. 23-25 2002, pp 357-362

[17] D. LeBlond, F. Owen, G. Gibson, C. Haas, A. Traver, "Performance Testing and Characterization of Advanced Construction Equipment", ASCE Journal of Construction Engineering and Management, 124(4), pp. 289-296, 1998

[18] K. Lin, C. Haas, "An Interactive Planning Environment for Critical Operations", ASCE Journal of Construction Engineering and Management, 122(3), pp. 212-222, 1996

[19] J. McLaughlin, S.V. Sreenivasan, C. Haas, K. Liapi, "Rapid Human-assisted Creation of Bounding Models for Obstacle Avoidance in Construction" accepted to Journal of Computer-aided civil and infrastructure engineering

[20] "Lasers Go into Overdrive, Pushed by Technology Gains", Engineering New Record, Sep. 16 2002, pp.54-55

[21] J. Neugebuer, "Virtually reality – More than just simulation." Industrial Robot, 19(3), 1992

[22] B. Sabata, F. Arman, J.K. Aggarwal, "Segmentation of 3D Range Images Using Pyramidal Data Structures", CVGIP: Image Understanding, 57(3), pp. 373-387, 1993

[23] D.G. Schweikert, "An Interpolation Curve Using Spline under Tension," Journal of Math. Phys., vol. 45, pp 312-317, 1996

[24] Stentz, J. Bares, S. Singh, P. Rowe, "A Robotic Excavator for Autonomous Truck Loading", Proceedings of IEEE/RSJ International Conference on Intelligent Robots and Systems , vol. 3, pp. 1885–1893, 1998

[25] W. Stone, G. Cheok, "LADAR Sensing Applications for Construction", Technical paper, National Institute of Standards and Technology, 2001

[26] W. Stone, G. Cheok, R. Lipman, "Automated Earthmoving Status Determination", Robotics 2000, ASCE Conference on Robotics for Challenging Environments, Albuquerque, NM, Feb. 28 – Mar. 2, 2000

[27] B.C. Vermuri, J.K. Aggarwal, "Representation and Recognition of Objects from Dense Range Maps," IEEE Trans. on Circuits and Systems, CAS-34(11), Nov. 1987

[28] B.C. Vermuri, A. Mitiche, J.K. Aggarwal, “Curvature-based Representation of Objects from Range Data,” Image and Vision Computing, 4(2), pp. 107-114, 1986

Vitae

Soon-Wook Kwon received the B.S. degree from Hongik University of Seoul, Korea, in 1992, the M.S. degree from Georgia Institute of Technology, Atlanta, GA, in 1999 and doing Ph.D. degree in Civil Engineering at The University of Texas at Austin. He has been working at Field Systems and Construction Automation laboratory of The University of Texas at Austin since he started his Ph.D. study in 2000. His research interests include automation and robotics in construction, machine vision, and interoperability in construction industry.

Frederic Bosche is completing double-degree studies including an Engineering degree from Ecole Centrale de Lille, France, and a M.S. degree from the University of Texas at Austin. He has been working at Filed Systems and Construction Automation laboratory of the University of Texas at Austin since he started his M.S. degree in 2002. His research interests include automation and robotic in construction and machine vision.

Changwan Kim received the B.S. degree from Chung-Ang University of Seoul, Korea, in 1998, the M.S. degree from University of California at Berkeley, CA, in 2000 and doing Ph.D. degree in Civil Engineering at The University of Texas at Austin. He has been working at Field Systems and Construction Automation laboratory of The University of Texas at Austin since he started his Ph.D. study in 2001. His research interests include automation and robotics in construction, machine vision, and breakthrough technologies in construction industry.

Carl T. Haas is the Liedtke Centennial Fellow and a Professor of Civil Engineering at The University of Texas at Austin. His research, teaching and consulting are in the areas of advanced construction and transportation technology, and construction workforce issues. He teaches courses in Construction Automation, Sensing in Civil Engineering, Heavy Construction,

Engineering Economics, Scheduling, and Project Management. His most recent research is in the areas of rapid local area sensing and modeling for construction automation, 3D scanning and analysis of aggregates, teleoperated robots for hazardous environments, critical construction operations planning, automated infrastructure maintenance, trenchless technologies, remote highway condition and incident detection, and construction workforce issues. He has received several research and teaching awards. He consults in the area of construction and transportation technology issues. He has over one hundred publications and serves on a number of professional committees such as the Construction Industry Institute Breakthrough Committee. He also directs the UT Construction Automation Laboratory. He is a member of IEEE Robotics and Automation Society (ROS), member of CIB Task Group 27 Human-Machine Technologies for construction sites 1997 to present, and member of board of directors International Association for Automation and Robotics in Construction - 1995 to present.

Katherine A. Liapi is Assistant Professor of Civil Engineering at The University of Texas at Austin. She received the B.S. degree from National Technical of Athens, Greece, in 1982, the M.S. degree from The University of Texas at Austin in 1988 and the Ph.D. degree at The University of Texas at Austin in 1994. She received several research and teaching awards. Her research interests include CAD application in design and construction, motion simulation in the design and construction of buildings, and daylight and natural ventilation simulation in buildings.